Angewandte Chemie
Eine Zeitschrift der Gesellschaft Deutscher Chemiker

Supporting Information

Parahydrogen Hyperpolarization Allows Direct NMR Detection of α-Amino Acids in Complex (Bio)mixtures

*Lisanne Sellies, Ruud L. E. G. Aspers, Martin C. Feiters, Floris P. J. T. Rutjes, and Marco Tessari**

anie_202109588_sm_miscellaneous_information.pdf

Supporting Information

Abstract: The scope of non-hydrogenative parahydrogen hyperpolarization (nhPHIP) techniques has been expanding over the last years, with the continuous addition of important classes of substrates. For example, pyruvate can now be hyperpolarized using the Signal Amplification By Reversible Exchange (SABRE) technique, offering a fast, efficient and low-cost PHIP alternative to Dynamic Nuclear Polarization for metabolic imaging studies. Still, important biomolecules such as amino acids have so far resisted PHIP, unless properly functionalized. Here, we report on an approach to nhPHIP for unmodified α-amino acids that allows their detection and quantification in complex mixtures at sub-micromolar concentrations. This method was tested on human urine, in which natural α-amino acids could be measured after dilution with methanol without any additional sample treatment.

DOI: 10.1002/anie.2021XXXXX

Table of contents

Experimental Procedures

Chemicals

The precursor complex [Ir(IMes)(COD)Cl] (COD = cyclooctadiene; IMes = 1,3-bis(2,4,6- trimethylphenyl)imidazole-2-ylidene) was synthesized according to a published method.[1] Ultrapure water (MilliQ) was generated by a Milli-Q academic water purification system with a Q-Gard® 2 purification pack and a Quantum® EX cartridge purchased by Millipore. p-H_2 was produced with a 2 L vessel embedded in a liquid nitrogen bath. Normal hydrogen (purity 5.0) was cooled down to 77 K in the presence of 100 mL of 4-8 MESH activated charcoal (Sigma-Aldrich). The resulting 51% p-H_2 was transported to an aluminum cylinder (Nitrous Oxides Systems, Holley Performance Products, Bowling Green, KY, USA)[2] with an adjustable output-pressure valve.

The other chemicals were purchased from Cambridge Isotope Laboratories (L-alanine-3-^{13}C), Fluka AG (L-cysteine, L-lysine monohydrochloride and L-valine), Fisher Scientific (L-arginine, methanol), J.T. Baker (ammonium chloride), Merck KGaA (potassium hydroxide), Sigma-Aldrich (creatinine, deuterated water, L-histidine, hydrochloric acid, methanol-d_4, (R)-(+)-α-methylvaline, piperidine, piperidine hydrochloride, potassium hydroxide, pyridine, sarcosine and sodium chloride), Sigma Chemical Company (L-alanine, L-asparagine, L-aspartic acid, L-glutamic acid, L-glutamine, glycine, L-isoleucine, L-leucine, L-methionine, L-phenylalanine, L-proline, L-serine, L-threonine, L-tryptophan and L-tyrosine), VWR International (urea) and used as supplied.

Sample preparation

Amino acid and their mixtures

18 stock solutions were prepared which contained 20 mM of an amino acid in MilliQ: L-alanine, L-arginine, L-asparagine, L-aspartic acid, L-glutamic acid, L-glutamine, glycine, L-isoleucine, L-leucine, L-lysine, (R)-(+)-α-methylvaline, L-phenylalanine, L-proline, sarcosine, L-serine, L-threonine, L-tryptophan or L-valine. L-tyrosine was dissolved in MilliQ at a concentration of 10 mM by increasing the pH to 11 with potassium hydroxide. To determine the chemical shifts of the α-amino acids, aqueous samples were prepared by mixing (one of the) above solutions (25 µL) with a NaCl solution (100 µL, 1 M) and MilliQ (375 µL). A 1 mM mixture of the above mentioned 19 amino acids was prepared by mixing 160 µL of L-tyrosine (10 mM) with 80 µL of each of the 18 amino acids (20 mM). This mixture was diluted 5.3 times with a NaCl solution in MilliQ (0.13 M). The relative amino acid concentrations were determined by thermal NMR. This mixture was further diluted in methanol to yield the 10 µM mixture which was used for quantification and the chemical shifts determination.

For the measurements in methanol-d_4, stock solutions of the 20 proteinogenic α-amino acids and sarcosine in MilliQ were prepared gravimetrically (20 mM, except for L-tryptophan, L-glutamic acid and L-aspartic acid: 10 mM and L-tyrosine: 2 mM). A 10 µM mixture for the assignment of the chemical shifts and a 1 µM mixture (see figure 4) were prepared from a mix of these solutions in methanol-d_4. Note that due to the dilution steps the water content in these mixtures is almost negligible (around 1.5 and 0.15 vol%, respectively). Similarly, the sample used for the exchange experiment was prepared from stock solutions in D_2O, with final concentrations of 1.5 µM of each of the 20 proteinogenic α-amino acids, sarcosine and (R)-(+)-α-methylvaline.

Urine

A urine sample was collected from a healthy volunteer. Informed consent was obtained for the experiment on this sample to be included in the article. All procedures were in accordance with the Helsinki Declaration of 1975, as revised in 2000.
Approval for the study was obtained from the Research Ethics Committee of the Faculty of Science of the Radboud University (Approval number: REC21111). The urine sample was collected using routine clinical collection protocols and stored at −80 °C.
Before performing the NMR measurement, the pH of the urine sample was adjusted to 9 with dropwise addition of 0.5 M NaOH. Subsequently, the sample was centrifuged at room temperature for 10 min (14100 RCF) to remove the sediment.

pH setting

The pH of the aqueous samples (individual amino acids, mixture of amino acids and urine) was iteratively adjusted with KOH and HCl solutions such that the pH of the resulting NMR sample containing 4.3 vol% of this solution in methanol was 10.3. pH measurements were carried out using the Thermo Scientific™ Orion™ ROSS™ Sure-Flow™ pH Electrode filled with a 3 M KCl solution. Note that a

pH of 10.3 measured with a pH meter calibrated on aqueous buffer solutions corresponds to a pH* (i.e. the pH defined in a 4.3 vol% H_2O, 95.7 vol% methanol solvent) of 11.3.[3]
To simplify this laborious procedure, a piperidine buffer consisting of piperidine and piperidinium chloride was used to set the pH in the methanol-water mixtures used in figure 3 (1.5 mM) and 5 (20 mM) of the main text. The pKa's of piperidine in water and methanol are respectively 11.07[4] and 11.22[5].

Water content and dilution series

A pool of ^{13}C-3-alanine, [Ir(IMes)(COD)Cl], pyridine and piperidine/piperidinium was mixed together with methanol-d_4 and D_2O such that the water content could be adjusted by varying the ratio between the latter two. The NMR sample contained 200 µM ^{13}C-3-alanine, 840 µM [Ir(IMes)(COD)Cl],15.1 mM pyridine and 20 mM piperidine/piperidinium. The water content was set between 1 and 50 vol%.

Four samples were prepared for the dilution series of the four amino acids (see figure 7) from a stock solution containing L-isoleucine (3.13 mM), L-arginine (3.19 mM), L-aspartic acid (3.15 mM), L-proline (3.24 mM), ammonium chloride (42.0 mM) and NaCl (205 mM) in MilliQ. This stock solution was diluted with MilliQ by a factor 1 (no dilution), 2, 4 and 8. The pH of these samples was adjusted to 10.9. After diluting another factor 20 with a mixture of catalyst and pyridine in methanol-d_4, the amino acid concentrations in the four NMR samples were approximately 21, 42, 86 and 174 µM with 4.9-5.3 vol% water.

NMR samples and bubble setup

A weighed mixture of pyridine, precursor complex, methanol/methanol-d_4 and a sample containing the amino acids was added into a quick pressure valve (QPV) NMR tube. The tube was connected to the in-house designed bubble setup (see figure S.1).[6,7] The mixture was flushed with nitrogen to remove dissolved oxygen, after which p-H_2 was bubbled through the sample. The tube was then placed in a 50°C bath for 7.5 minutes to simultaneously speed up the hydrogenation (activation) of the catalyst and allow reaching the thermodynamic equilibrium for amino acid binding to the catalyst. Subsequently, the tube was cooled down to 5 °C and re-pressurized before placing the sample in the NMR spectrometer at 5 °C. To determine the kinetically favored binding mode of the α-amino acids, amino acid addition was performed after catalyst activation at 50 °C.

The NMR samples contained 0.83-0.88 mM catalyst and 15-15.7 mM pyridine, in a ratio 1:18. In some cases, the catalyst concentration was halved, for instance for the dilution series of the four amino acids.

At the beginning of every transient of the hydride nhPHIP 1D and 2D nhPHIP-ZQ NMR experiments, p-H_2 was bubbled through the sample. This bubble block consists of four steps. In the first step (typically 250 ms) the pressure in the NMR tube is reduced via the 'vent-line' from 5 to 4 bars against an adjustable relief valve calibrated at 4 bar. Bubbling p-H_2 at 5 bars pressure (typically 0.5 – 3.0 s) through the solution using the 'bubble-line', takes place during the second step. This is followed by a delay (ca. 250 ms) in which pressure is applied on top of the liquid level, 'back pressure', to stop the bubbling. The final delay (0.5 s) before the first excitation pulse stabilizes the solution, preventing signals distortion.

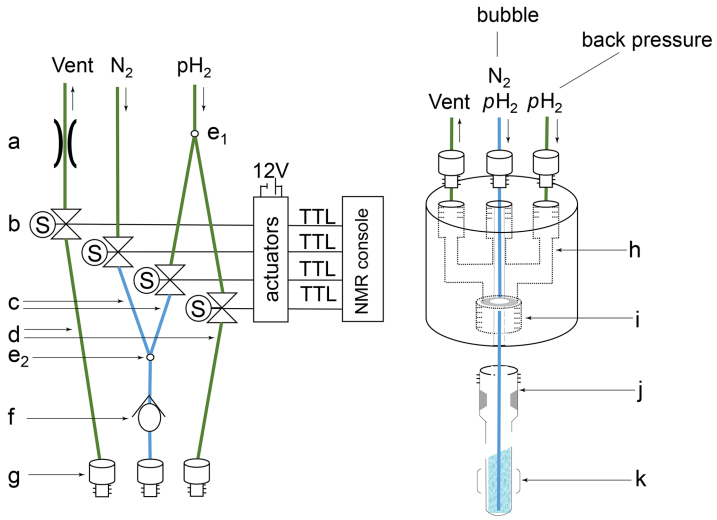

Figure S.1. Schematic representation of the gas–liquid reaction set-up. Left: **a** variable pressure relief valve, set to 4 bar; **b** solenoid valves controlled via TTL lines powered by an external 12 V source and timed via trigger commands in the pulse sequence taking care of a controlled supply of nitrogen and parahydrogen **c** 1/16″ O.D. PEEK tubing with 0.010″ I.D. (blue); **d** 1/16″ O.D. PEEK tubing with 0.030″ I.D. (green); **e** Y splitter: (**e**$_1$) splitting 5 bar p-H_2 source into a "bubble" and a "back pressure" line, (**e**$_2$) combining 5 bar N_2 and p-H_2 sources into a joined bubble line; **f** one-way valve; **g** tube fitting UNF 10-32 connectors. Right: **h** headpiece connecting the PEEK tubing holding the 7″ thin wall QPV NMR tube; **i** UNF 7/16-20 thread holding the QPV NMR tube – using a 2 mm silicon

disc on top of the tube to close off the system; **j** Wilmad 7″ thin wall QPV NMR tube; **k** area of detection with the bubble line centered down to the bottom of the NMR tube. Figures also presented in ref. 8.

NMR experiments

NMR spectra were typically acquired at 278.2 K on an Agilent Unity INOVA 500 MHz spectrometer equipped with a cryo-cooled HCN probe with a shielded z-gradient coil.

1D NMR spectra of alanine (figure 3), selectively ^{13}C-labeled at the methyl position, were acquired under equilibrium conditions employing an (^{13}C, ^{1}H) HSQC pulse sequence for ^{13}C-filtering. Spectra were typically acquired recording 32 transients, with a recovery delay of 7 s and a spectral width of 10000 Hz.

Hydride nhPHIP 1D NMR spectra were typically acquired with 16 or 32 transients in an acquisition time of one or three minutes using a SEPP (selective excitation of polarization using PASADENA)[9,10] pulse scheme (see figure S.2A), centered at -26.1 ppm.

2D nhPHIP-ZQ NMR (see figure S.2B) spectra were typically acquired with spectral widths of 1800 and 6000 Hz in the indirect (t_1) and acquisition (t_2) dimension, respectively, with 600(t_1, real)×3000(t_2, complex) points (note that (most) signals are folded in the indirect dimension because their ZQ frequency is larger than the spectral width). The spectral width and number of points in the indirect dimension were reduced for the 1 µM mixture (1625 Hz, 400 points) and the dilution series of the four amino acids (1040 Hz, 120 points). Two transients were collected for each increment. Similarly, a 2D nhPHIP-ZQ exchange NMR spectrum (see figures S.9 and S.10) was recorded where the delay τ (see figure S.2B) was extended to 250 ms. This spectrum was acquired with spectral widths of 1800 and 6000 Hz in the indirect (t_1) and acquisition (t_2) dimension, respectively, with 400(t_1, real)×3000(t_2, complex) points and four transients were collected for each increment.

The pulse sequence of the 2D thermal-ZQ NMR experiment (used for figure S.5) is similar to the one of the 2D nhPHIP-ZQ except for the beginning (a to b, figure S.2B). The first 90° pulse creates in-phase magnetization from the longitudinal magnetization of the hydrides (present at Boltzmann equilibrium). A spin echo block with a selective reburp pulse converts the in-phase to anti-phase magnetization, which becomes multiple quantum coherence after a 45° pulse. Then, b to f of the 2D nhPHIP-ZQ NMR experiment follows (see figure S.2B). A 2D thermal-ZQ NMR spectrum was acquired with spectral widths of 600 and 6000 Hz in the indirect (t_1) and acquisition (t_2) dimension, with 80(t_1, real)×6000(t_2, complex) points. 64 transients were collected for each increment.

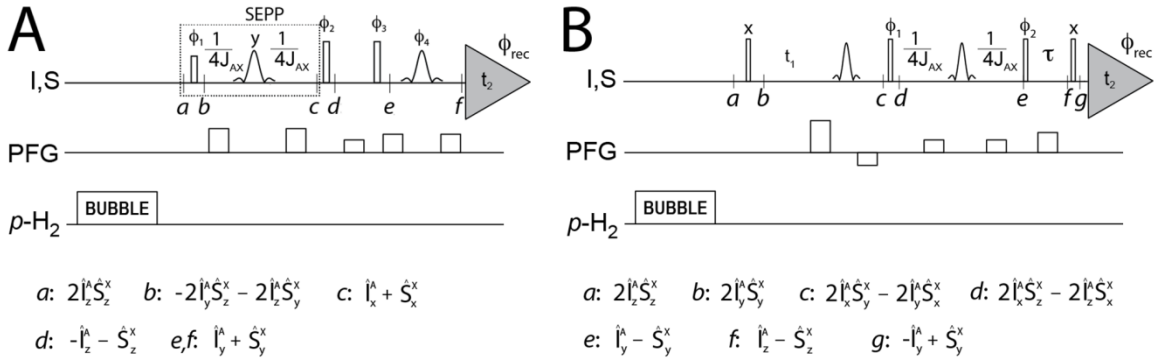

Figure S.2. A Pulse scheme to acquire a hydride 1D nhPHIP NMR spectrum (based on a Selective Excitation of Polarization using PASADENA (SEPP) pulse scheme).[9,10] Phase cycling: ϕ_1: x, -x; ϕ_2: 2(y), 2(-y); ϕ_3: 4(x), 4(y), 4(-x), 4(-y); ϕ_4: 4(y), 4(-x), 4(-y), 4(x); ϕ_{rec}: x,-x,-x,x, y,-y,-y,y, -x,x,x,-x, -y,y,y,-y. The transmitter offset is set to –25.014 ppm. **B** Pulse scheme used for the acquisition of a 2D nhPHIP-ZQ NMR spectrum of the hydrides. Phase cycling is implemented as follows: ϕ_1 = x,x,-x,-x; ϕ_2 = x,-x; ϕ_{rec} = x,-x,-x,x. The transmitter offset is set to –25.014 ppm. **A** and **B** Bubbling p-H_2 in the sample (between 0.5 and 3 s) occurs under spectrometer control at the beginning of each transient. The small and large rectangular pulses indicate 45° and 90° pulses, respectively, while shaped pulses represent selective reburp pulses with a bandwidth of 6000 Hz. J_{AX} denotes the average inter-hydrides scalar coupling constant (8.9 Hz). The acquisition time is indicated by t_2. Relevant terms of the density operator at different time points are indicated. Figure also presented in ref. 7.

The 1D data sets were processed and the spectra were analyzed with ssNake[11] and iNMR (http://www.inmr.net). The 2D data sets were processed with NMRPipe[12] using 72 degree shifted squared sine-bell apodization in t_2, and 90 degree shifted sine-bell apodization in t_1, prior to zero filling to 4096(t_1, real)×32768(t_2, complex) points and Fourier transformation. Nmrglue[13] and iNMR (http://www.inmr.net) were used to analyze the 2D spectra.

Results and Discussion

Identification of the “axial”, “axial/equatorial” and “amino” complexes

Figure S.3 shows hydride 1D thermal NMR spectra measured before and after warming a sample containing glycine, activated Ir-IMes catalyst and pyridine to 50 °C for 7.5 minutes. Three pairs of hydride signals for glycine were observed indicating that there are three binding forms of the α-amino acids to the Ir-IMes catalyst in an excess of the co-substrate pyridine.

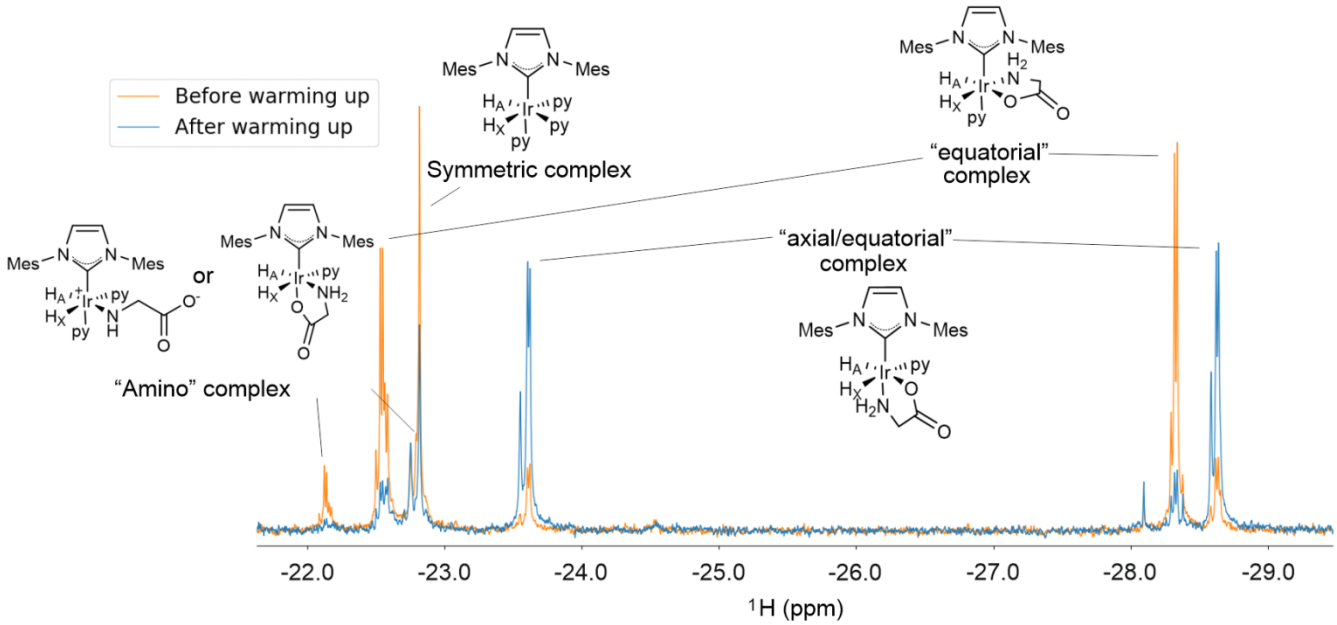

Figure S.3. Hydride 1D thermal NMR spectra of a sample of glycine, activated Ir-IMes catalyst and pyridine. These spectra were recorded before and after the sample was warmed up to 50°C for 7.5 minutes.

The highest pair of hydride signals before warming up were assigned to an “equatorial” binding of the α-amino acids, since these hydride signals are barely enhanced by nhPHIP, see figure S.4.

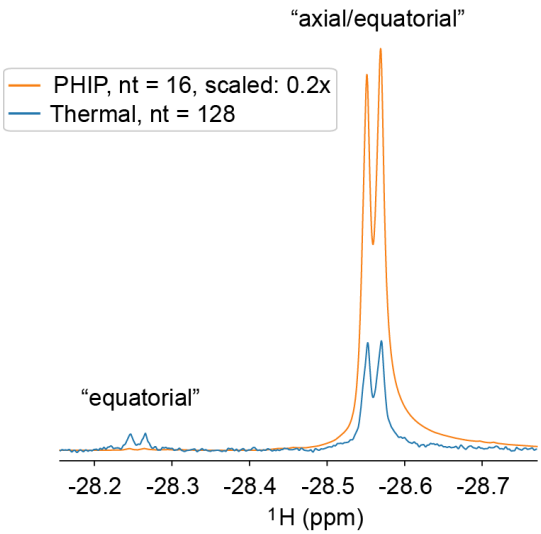

Figure S.4. Hydride 1D nhPHIP and thermal NMR spectra of a glycine sample (0.34 mM) in the presence of Ir-IMes catalyst (0.84 mM) and pyridine (15.6 mM) in a H_2O:methanol-d_4 = 4.6:95.4 vol% mixture. These spectra were recorded after warming the sample up to 50°C for 7.5 minutes. Note that the nhPHIP and thermal spectra were recorded with a different number of transients (nt) and that the nhPHIP spectrum is scaled by a factor 0.2. Although a large nhPHIP signal is observed for the ”equatorial/axial” complex, hardly any nhPHIP signal is obtained for the “equatorial” complex.

This means that no substrates are dissociating from this complex on the NMR timescale; otherwise, p-H_2 could be exchanged leading to nhPHIP, since p-H_2 exchange is an associative process that occurs after substrate dissociation according to the dissociative model for H_2 association.[14] The axially bound ligands do generally not exchange on the NMR timescale, due to their stronger interaction with the iridium center.[15] On the other hand, the exchange in the equatorial plane can be blocked by a tight bidentate binding amino acid. This assignment is supported by the 2D thermal-ZQ NMR spectrum showing one of the hydride signals of the "equatorial" glycine complex, see figure S.5:

- The chemical shift of this hydride signal is -28.3 ppm, which falls in the region where the hydrides trans to a carboxyl group in Ir-IMes α-carboxyimine complexes were found to resonate.[16]
- The signal consists of three components, of which the integral ratios match those expected for NH_2, NHD and ND_2 in the mixed H_2O/methanol-d_4 solvent. We attribute this structure of the hydride signal, therefore, to an isotope effect caused by the protonation/deuteration of the amino group. This indicates that the H/D exchange on this group is slowed down when it binds to the iridium center.

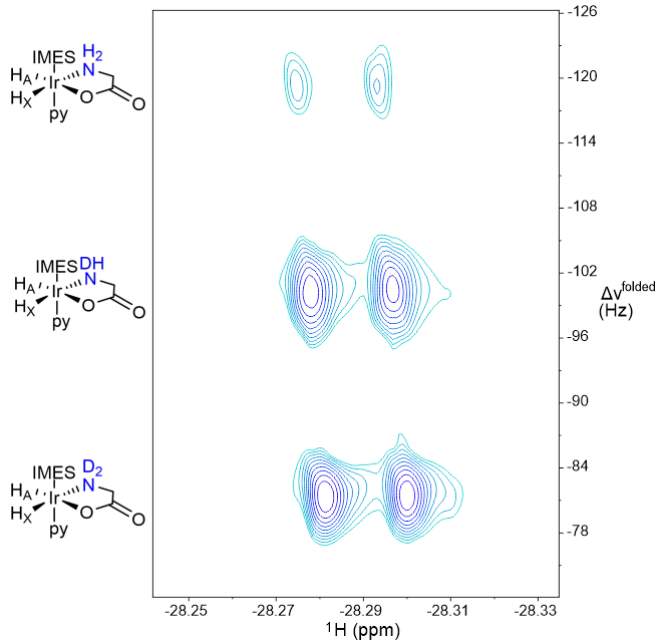

Figure S.5. 2D thermal-ZQ NMR spectrum of glycine in a H_2O:methanol-d_4 = 11.3:88.7 vol% mixture recorded at 10°C without warming the glycine sample up before the measurement. This spectrum shows the high field hydride of the "equatorial" glycine complexes, which consists of three components due to a H/D isotope effect. The proposed molecular structures of the glycine complexes are indicated.

After heating the sample to 50°C for 7.5 minutes, the hydride signals assigned to the "axial/equatorial" complex dominate (see figure S.3). Their assignment is derived from a 2D nhPHIP-ZQ spectrum (figure S.6) showing one of the hydride signals of this complex for alanine:

- This hydride signal has a chemical shift of -28.6 ppm, which falls again in the region where hydrides trans to a carboxyl group in Ir-IMes α-carboxyimine complexes were found to resonate.[16]
- Similar to the case of the "equatorial" complex, the hydride signal consists of three components, with a relatively large separation ($\Delta\nu \approx 11.5$ Hz). However, the integral ratio of these three components does not correspond to the concentration ratio of protons and deuterons. We have attributed this structure of the hydride signal to an isotope effect caused by the partial deuteration of the ortho protons of the co-substrate pyridine. Such a H/D exchange can be catalyzed by the Ir-IMes catalyst, as reported in literature for pyridine and other substrates.[17-19]
- Further, minor contributions with a much smaller line separation ($\Delta\nu \approx 4$ Hz) are observed, which are attributed to an isotope effect caused by the protonation/deuteration of the amino group. This effect is weaker than the one observed for the "equatorial" complexes (see figure S.5), which indicates that the amino group is bound to a chemically different position in the complex, in other words, the axial position.

Together, these observations allow the assignment of the nhPHIP active complexes to "axial/equatorial" complexes.

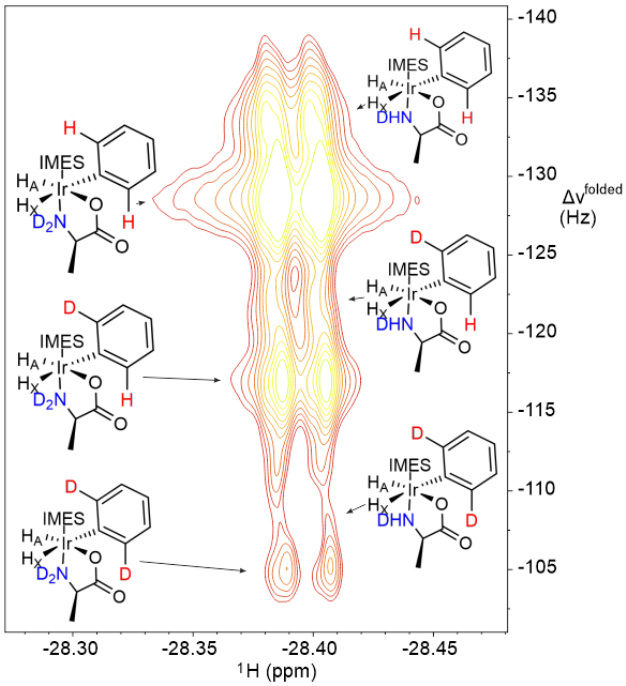

Figure S.6. 2D nhPHIP-ZQ NMR spectrum of alanine in a H_2O:methanol-d_4 = 4.8:95.2 vol% mixture. One hydride signal of an "axial/equatorial" alanine complex is shown that consists of (at least) six components. The proposed molecular structure of the catalyst with its ligands are indicated for each signal component.

Furthermore, small signals of a third complex are observed in the hydride spectra, see figure S.3. Two observations are made that can guide their assignment:

- These signals display an isotope effect similarly as the "equatorial" complex signals, indicating that the nitrogen group binds in the equatorial plane.
- In contrast to the "equatorial" complexes, both hydride signals resonate around -22.5 ppm, indicating that the carboxyl group is not bound in the equatorial plane.

Since the hydrides chemical shifts are close to those observed for the complex of ammonia with pyridine as co-substrate (-22.24, -22.66), a similar configuration for this complex, with the amino acid binding monodentate to the catalyst is possible. Alternatively, a bidentate binding involving the amino group in the equatorial plane and the carboxyl group in the axial position should be considered. We refer to this complex as "amino" in the main text.

Assignment of the "axial/equatorial" α-amino acid complexes in methanol-d_4

Table S.1. Chemical shifts of the hydride signals of the "axial/equatorial" amino acid complexes

Amino acid	δ H_X (ppm)	δ H_A (ppm)
Alanine	-23.54	-28.38
	-23.61	-28.21
Arginine[a]	-23.62	-28.25
	-23.45	-28.35
Asparagine	-23.58	-28.24
	-23.44	-28.60
Glutamine	-23.60	-28.32
	-23.64	-28.20
Glycine	-23.55	-28.55
Isoleucine	-23.70	-27.92
	-23.75	-28.07
Leucine	-23.58	-28.08
	-23.61	-28.21
Lysine[a]	-23.65	-28.14
	-23.59	-28.31
α-methylvaline	-23.78	-27.78
	-23.81	-27.50
Phenylalanine	-23.44	-28.55
	-23.71	-28.35
Proline	-23.23	-28.32
	-23.69	-28.39
Sarcosine	-23.44	-28.86
	-23.27	-28.70
Serine	-23.65	-28.29
	-23.55	-28.51
Threonine	-23.73	-28.20
	-23.53	-28.38
Tryptophan	-23.85	-28.31
	-23.44	-28.52
Tyrosine	-23.78	-28.34
	-23.48	-28.53
Valine	-23.76	-28.06
	-23.67	-28.01

[a] These chemical shifts are sensitive to minor variations in the sample conditions (e.g. pH, water content)

Table S.1 lists the hydride chemical shifts derived from 2D nhPHIP-ZQ spectra recorded for (mixtures of) the amino acids in methanol-d_4. The hydrides resonances for the complexes formed by aspartic and glutamic acid and, to a lesser extent by lysine and arginine appear to be extremely sensitive to minor variations in the sample conditions (e.g. pH, water content). For this reason, particularly for the acidic residues, it has proven hard to determine reproducible chemical shifts for the corresponding hydrides.
Note further that cysteine, histidine and methionine are not present in this table. The hydrides for the complexes formed by these three amino acids resonate in a different region of the 2D nhPHIP-ZQ spectrum. In addition, the binding modes of these amino acids seem to be more complex, with a likely involvement of the side chains (thiol, imidazole and thiolester). The structures of the resulting complexes are still under investigation.

Exchange between diastereoisomers probed via 2D nhPHIP-ZQ exchange experiment

As can be noted in table S.1, all listed amino acids give rise to two pairs of hydride signals arising from “axial/equatorial” binding, except for glycine. This can be attributed to the formation of two diastereoisomers upon association of the chiral amino acids to the Ir-IMes complex, as illustrated in figure S.7A. Note that in case of sarcosine this chiral center is created upon binding, see figure S.7B.

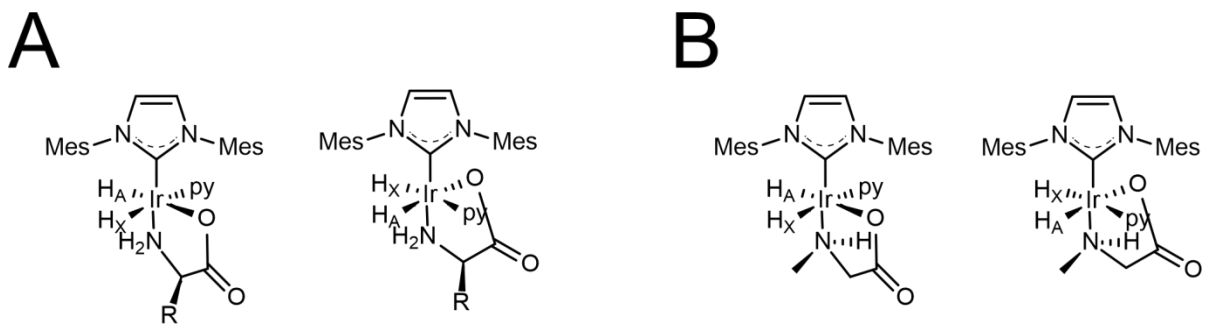

Figure S.7. A The two diastereomeric complexes formed for the chiral α-amino acids in an excess of the co-substrate pyridine, with R indicating the side chain of the amino acid. **B** The two diastereoisomers formed upon binding of sarcosine to the Ir-IMes complex in an excess of the co-substrate pyridine.

Pyridine dissociation/association plays a crucial role for the binding of fresh p-H_2 to these amino acid complexes. In fact, according to the dissociative model for H_2 binding, formation of the intermediate (2) is required for the association of a new p-H_2 molecule to the iridium catalyst (see figure S.8). Note that this intermediate is the same for both diastereomeric complexes, implying the same nhPHIP efficiency for the corresponding hydrides. Therefore, differences in the hydrides nhPHIP enhancements between the two diastereoisomers must primarily reflect their relative population ratio.

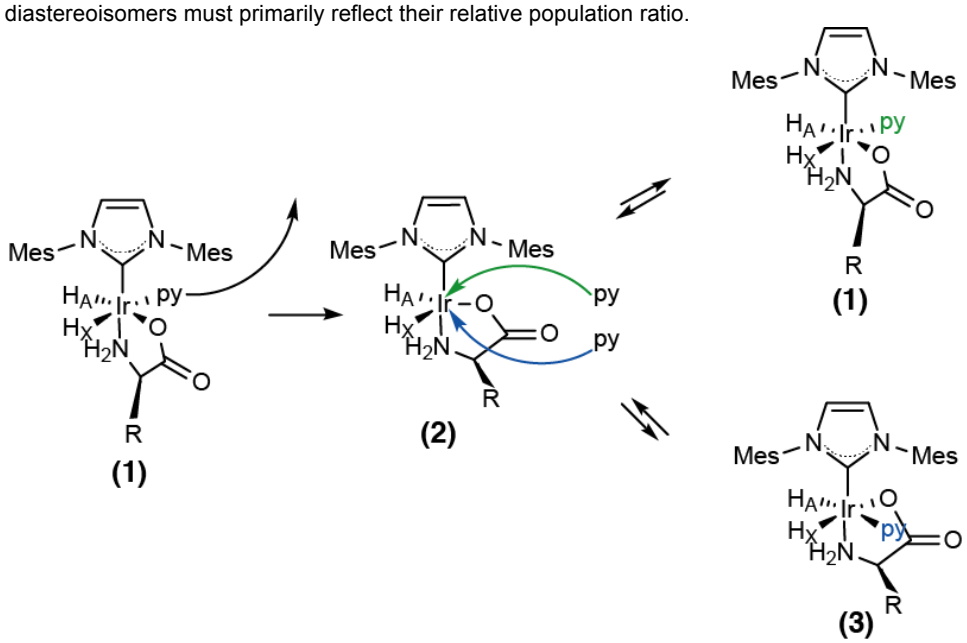

Figure S.8. Interconversion between the two diastereomeric amino acid complexes caused by pyridine dissociation/association. The starting complex is one of the diastereoisomers (1), which is converted into the intermediate (2), where pyridine can reassociate forming the same diastereoisomer (1) or the other (3).

The rapid interconversion sketched in figure S.8 can be observed by measuring a 2D nhPHIP-ZQ NMR experiment of the hydrides complexes in which the z-filter delay τ (see figure S.2B) is extended to 250 ms. The resulting 2D spectrum for a mixture of 22 α-amino acids at 1.5 μM in methanol-d_4 is shown in figure S.9. The dashed arrows indicate the hydrides magnetization transfer pathway between the two diastereomeric complexes of isoleucine.

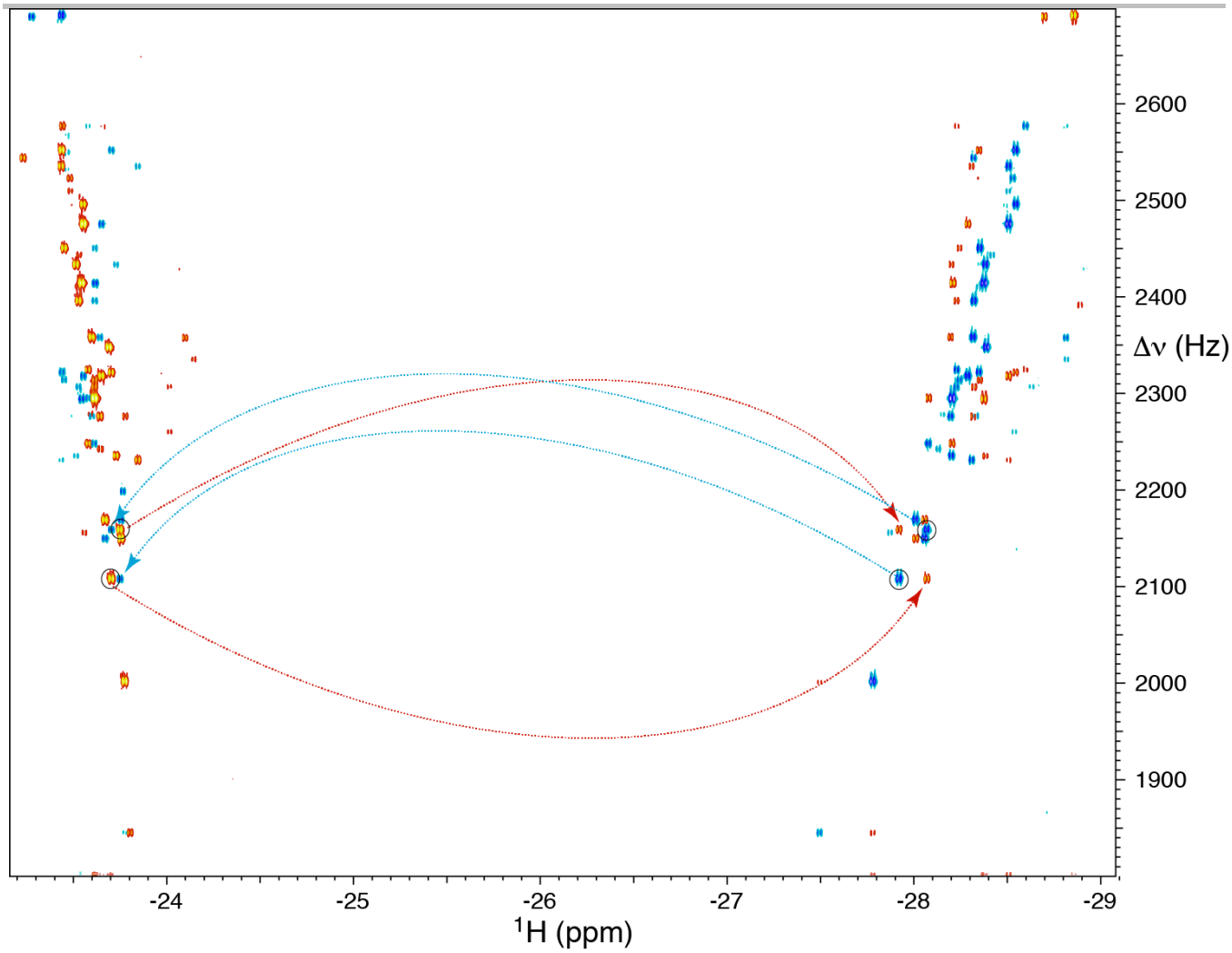

Figure S.9. 2D nhPHIP-Zero-Quantum Exchange hydrides' spectrum of a mixture of 20 proteinogenic α-amino acids, sarcosine and α-methylvaline at 1.5 μM in methanol-d_4. The dashed arrows illustrate the magnetization transfer associated to pyridine dissociation/association from/to the isoleucine complexes.

The high field region of this 2D spectrum is shown in figure S.10, with typical rectangular patterns that can be used to identify diastereomeric pairs. Note that for the signals of proline, marked with an asterisk, no transfer peaks are observed, indicating a much slower/absent pyridine exchange process. Interestingly, also a large difference in nhPHIP signal integrals is observed between the proline diastereomeric complexes, despite their comparable concentration in solution.

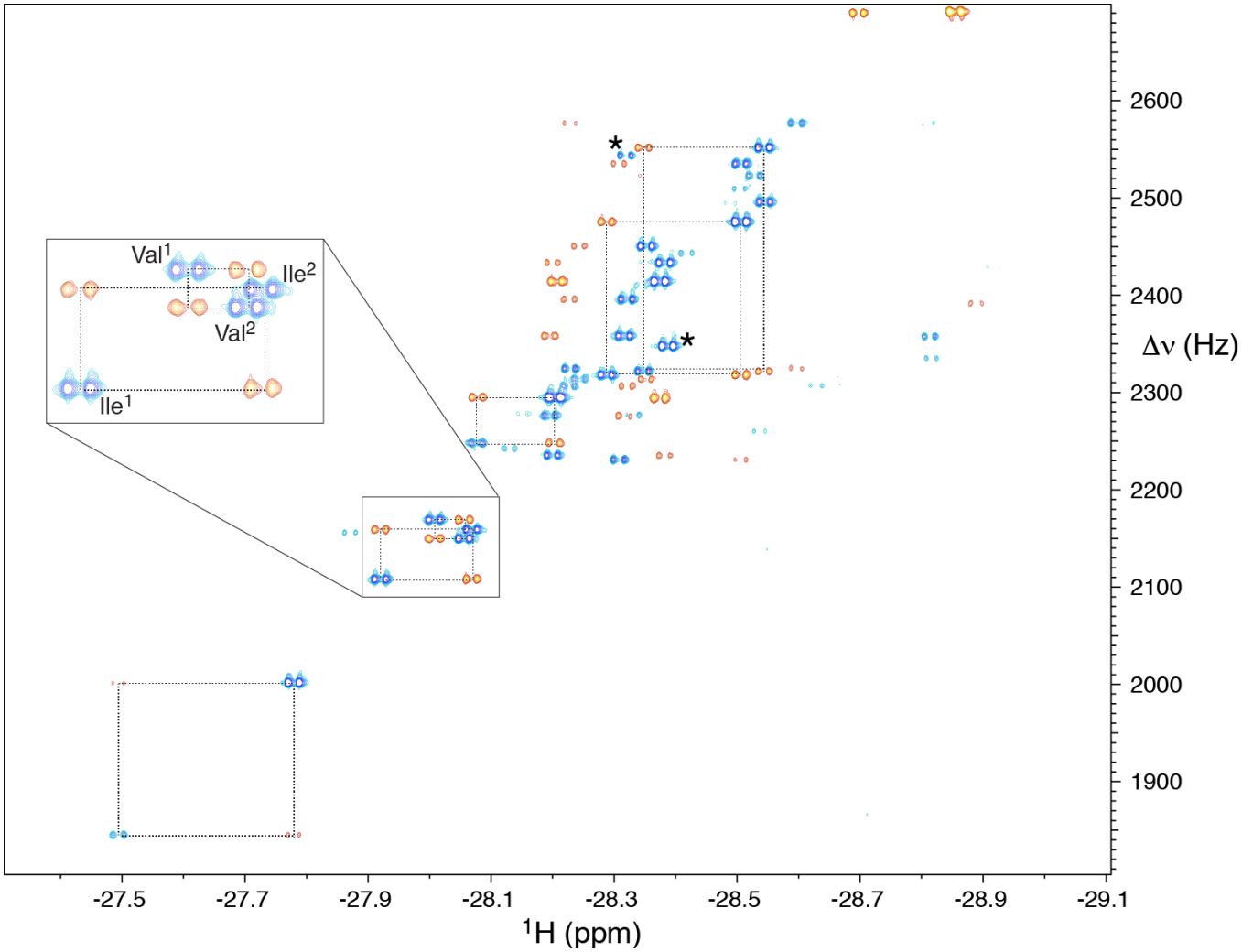

Figure S.10. High field region of the spectrum shown in figure S.9 displaying the transfer patterns that can be used to identify diastereomeric pairs. The asterisks indicate the proline signals, for which no exchange signals are observed.

Temperature dependence of nhPHIP for α-amino acids

The quality of nhPHIP-NMR hydrides spectra of α-amino acids complexes is strongly influenced by the temperature. The optimal setting was determined by analyzing the effect of temperature on the hydrides signals. Figure S.11 shows the high field hydride signal of one of the isoleucine complexes acquired at different temperatures between 5 and 25 °C. Note that at 25 °C, the signal is barely visible, which is likely due to a fast pyridine exchange in the "axial/equatorial" complexes. The signal becomes sharper as the measurement temperature is lowered, indicating an optimum for the α-amino acids complexes between 5 and 10 °C. We decided to measure at 5 °C to optimize the spectral resolution in the 2D nhPHIP-ZQ NMR spectra. The decay constant of the ZQ coherence is, in fact, primarily determined by the dissociation rate of pyridine. Therefore, despite the slight increase in viscosity at lower temperature, the line widths reduce upon lowering the temperature from 5 to 10°C due to the slower pyridine exchange.

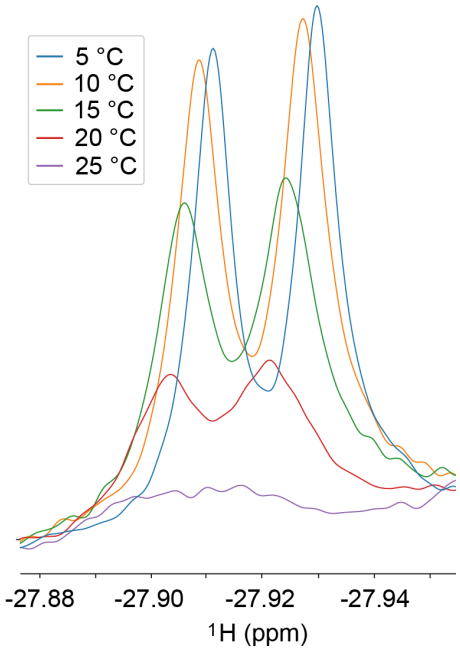

Figure S.11. High field nhPHIP-NMR signal of one of the diasteroisomers of isoleucine in methanol-d_4 measured at five temperatures between 5 and 25 °C.

2D nhPHIP-ZQ NMR spectrum of human urine after 20-fold dilution in methanol

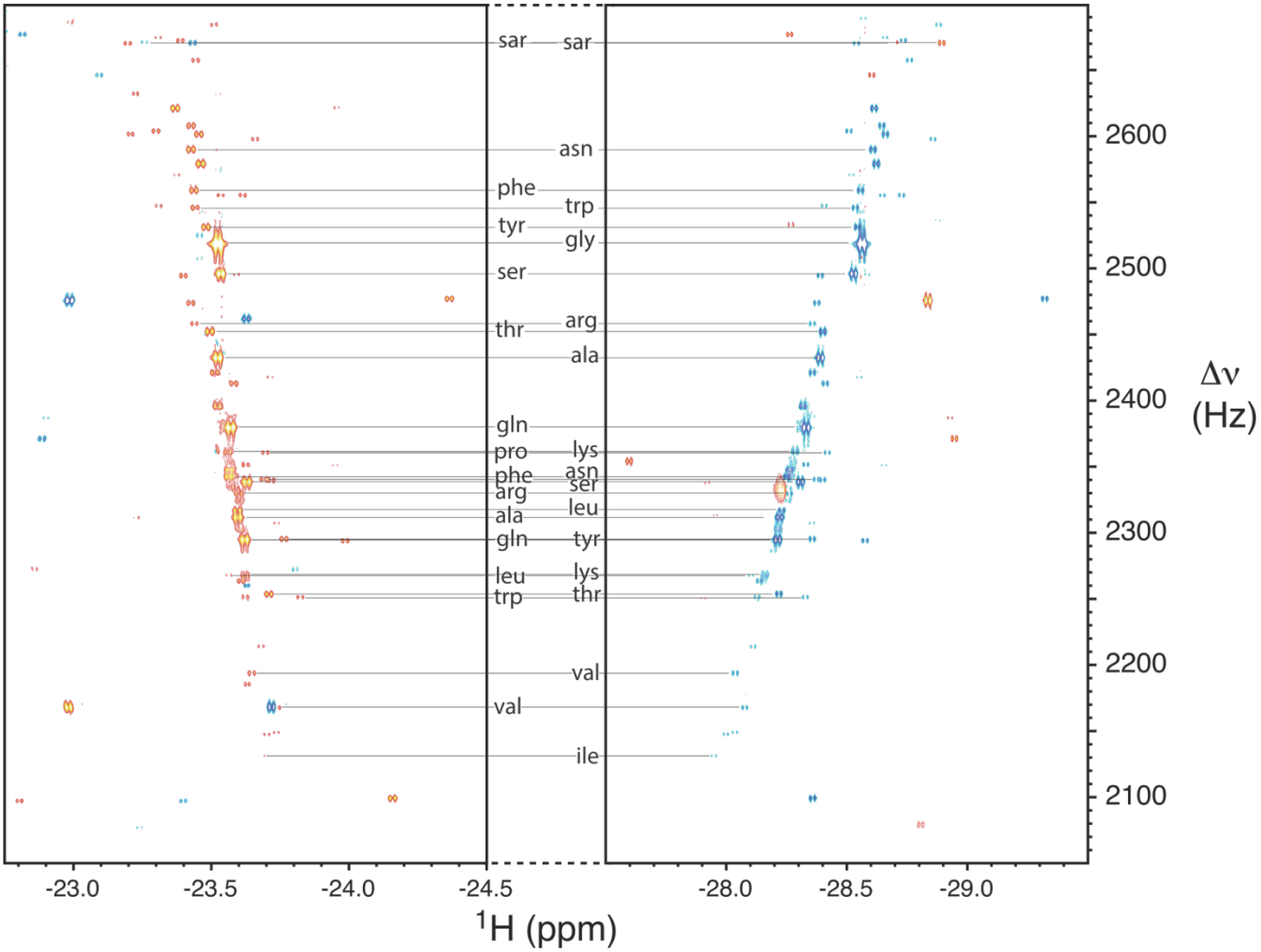

Figure S.12. 2D nhPHIP-ZQ NMR spectrum of a sample of 4.6 vol% human urine in methanol, acquired at 500 MHz ^{1}H resonance frequency, in the presence of 0.88 mM Ir-IMes catalyst and 15.8 mM pyridine as co-substrate. The experiment was recorded at 5 °C in ca. 40 minutes. The assignment of the hydride resonances of several amino acids is indicated.

Figure S.12 shows the 2D nhPHIP-ZQ NMR spectrum of a sample of 20 fold diluted human urine in methanol. Hydride resonances for 16 of the 19 α-amino listed in table S.2 could be assigned. No signals for α-methylvaline were observed. Further, aspartic acid and glutamic acid could not be assigned. This is attributed to their extreme sensitivity to minor variations in the sample conditions, such as the pH.

Assignment of the "axial/equatorial" α-amino acid complexes in 5 vol%-95 vol% water-methanol

Table S.2. Chemical shifts of the hydride signals of the "axial/equatorial" amino acid complexes.

Amino acid	δ H_X (ppm)	δ H_A (ppm)
Alanine	-23.52	-28.39
	-23.59	-28.22
Arginine	-23.43	-28.35
	-23.60	-28.25
Asparagine	-23.42	-28.60
	-23.56	-28.24
Aspartic acid	-23.46	-28.49
	-23.58	-28.10
Glutamic acid	-23.58	-28.25
	-23.62	-28.12
Glutamine	-23.57	-28.33
	-23.62	-28.21
Glycine	-23.52	-28.56
Isoleucine	-23.73	-28.08
	-23.68	-27.94
Leucine	-23.59	-28.22
	-23.56	-28.10
Lysine	-23.55	-28.28
	-23.61	-28.16
α-methylvaline	-23.76	-27.78
	-23.78	-27.52
Phenylalanine	-23.43	-28.55
	-23.69	-28.37
Proline	-23.21	-28.32
	-23.69	-28.41
Sarcosine	-23.25	-28.71
	-23.43	-28.89
Serine	-23.53	-28.52
	-23.62	-28.30
Threonine	-23.49	-28.40
	-23.70	-28.21
Tryptophane	-23.44	-28.53
	-23.82	-28.32
Tyrosine	-23.48	-28.54
	-23.76	-28.35
Valine	-23.64	-28.03
	-23.73	-28.07

Table S.2 lists the chemical shifts obtained from a 2D nhPHIP-ZQ NMR spectrum of a mixture of these amino acids in a H_2O:methanol-d_4 = 4.8:95.2 vol% mixture. The hydride signals were, therefore, first assigned by measuring these α-amino acids one by one in samples with a similar solvent composition.

Comparison of nhPHIP efficiency for different α-amino acids

A 2D nhPHIP-ZQ spectrum of 19 α-amino acids in a 4.8 vol%-95.2 vol% water-methanol solution was used to quantitatively compare the nhPHIP hydrides signals among the amino acid complexes. For each diastereomeric pair of complexes the sum of the hydrides integrals was calculated and the result was normalized with respect to the analytical concentration of the corresponding amino acid. The normalized integrals are reported in Table S.3 with respect to the normalized integral of glycine, taken as a reference.

Table S.3. Normalized nhPHIP integrals with respect to the normalized nhPHIP integral of glycine obtained from a 2D nhPHIP-ZQ NMR spectrum of a mixture of these amino acids in a H_2O:methanol-d_4 = 4.8:95.2 vol% mixture.

Amino acid	(Norm. Integ.)/(Norm. Integ. for Gly)
Glycine	1.0
Sarcosine	1.0
Alanine	1.1
Valine	1.1
Leucine	0.9
Isoleucine	1.1
Serine	0.6
Threonine	0.6
Tyrosine	0.6
Phenylalanine	0.8
Tryptophane	0.5
Lysine	0.6
Arginine	0.7
Aspartic acid	0.6
Glutamic acid	0.8
Asparagine	0.2
Glutamine	0.9
α-methylvaline	1.6
proline	1.6

The hydrides integrals normalized with respect to concentration allow a comparison of the nhPHIP efficiency between different amino acids. Interestingly, the observed normalized integrals seem to correlate with the properties of the amino acids side chain. We have attempted to group the amino acids in table S.3 according to the side chains properties. Note that in most cases, very similar normalized integrals are observed within each class. This observation suggests that a comparison of nhPHIP integrals for amino acids of the same class should provide a good estimate of their concentration ratio.

References

[1] R. A. Kelly III, H. Clavier, S. Giudice, N. M. Scott, E. D. Stevens, J. Bordner, I. Samardjiev, C. D. Hoff, L. Cavallo, S. P. Nolan, *Organometallics* **2007**, *27*, 202-210.

[2] B. Feng, A. M. Coffey, R. D. Colon, E. Y. Chekmenev, K. W. Wadell, *J. Magn. Reson.* **2012**, *214*, 258-262.

[3] W. Gelsema, C. De Ligny, A. Remijnse, H. Blijleven, *Recl. Trav. Chim. Pays-Bas* **1966**, *85*, 647-660.

[4] E. L. Miguel, P. L. Silva, J. R. Pliego, *J. Phys. Chem. B* **2014**, *118*, 5730–5739.

[5] H. Hall Jr, *J. Am. Chem. Soc.* **1957**, *79*, 5441–5444.

[6] N. Eshuis, R. L. E. G. Aspers, B. J. A. van Weerdenburg, M. C. Feiters, F. P. J. T. Rutjes, S. S. Wijmenga, M. Tessari, *Angew. Chem. Int. Ed.* **2015**, *54*, 14527– 14530.

[7] L. Sellies, I. Reile, R. L. E. G. Aspers, M. C. Feiters, F. P. J. T. Rutjes, M. Tessari, *Chem. Commun.* **2019**, *55*, 7235–7238.

[8] L. Sellies, R. L. Aspers, M. Tessari, *Magn. Reson.* **2021**, *2*, 331–340.

[9] H. Sengstschmid, R. Freeman, J. Barkemeyer , J. Bargon, *J. Magn. Reson., Ser. A* **1996**, *120*, 249-257.

[10] J. Barkemeyer, J. Bargon, H. Sengstschmid, R. Freeman, *J. Magn. Reson., Ser. A* **1996**, *120*, 129-132.

[11] S. van Meerten, W. Franssen, A. Kentgens, *J. Magn. Reson.* **2019**, *301*, 56-66.

[12] F. Delaglio, S. Grzesiek, G. W. Vuister, G. Zhu, J. Pfeifer, A. Bax, *J. Biomol. NMR* **1995**, *6*, 277-293.

[13] J. J. Helmus and C. P. Jaroniec*, J. Biomol. NMR* **2013**, *55*, 355-367.

[14] M. J. Cowley, R. W. Adams, K. D. Atkinson, M. C. R. Cockett, S. B. Duckett, G. G. R. Green, J. A. B. Lohman, R. Kerssebaum, D. Kilgour, R. E. Mewis, *J. Am. Chem. Soc.* **2011**, *133*, 6134–6137.

[15] B. J. van Weerdenburg, A. H. Engwerda, N. Eshuis, A. Longo, D. Banerjee, M. Tessari, C. F. Guerra, F. P. Rutjes, F. M. Bickelhaupt, M. C. Feiters, *Chem.-Eur. J.* **2015**, *21*, 10482-10489.

[16] B. J. Tickner, R. O. John, S. S. Roy, S. J. Hart, A. C. Whitwood, S. B. Duckett, *Chem. Sci.* **2019**, *10*, 5235-5245.

[17] D. A. Barskiy, K. V. Kovtunov, I. V. Koptyug, P. He, K. A. Groome, Q. A. Best, F. Shi, B. M. Goodson, R. V. Shchepin, A. M. Coffey, K. W. Waddell, E.Y. Chekmenev, *J. Am. Chem. Soc.* **2014**, *136*, 3322-3325.

[18] J. A. Brown, S. Irvine, A. R. Kennedy, W. J. Kerr, S. Andersson, G. N. Nilsson, *Chem. Commun.* **2008**, 1115-1117.

[19] G. N. Nilsson and W. J. Kerr, *J. Labelled Compd. Radiopharm.* **2010**, *53*, 662-667.